Microstructure evaluation of $MoSi_2$ based composite materials by SANS investigations

B. Ballóková[1]*, J. Šaroun[2,3], M. Besterci[1], P. Hvizdoš[1]

[1] *Institute of Materials Research SAS, Watsonova 47, 043 53 Košice, Slovak Republic*
[2] *Nuclear Physics Institute, v.v.i., ASCR 250 68 Řež, Czech Republic*
[3] *Research Centre Řež, Ltd., 250 68 Řež, Czech Republic*

Received 5 November 2008, received in revised form 4 July 2009, accepted 23 September 2009

Abstract

The paper deals with measurement of the microstructure parameters of monolithic $MoSi_2$ and $MoSi_2$ based composites with different volume fractions of secondary particles (SiC, Si_3N_4). Distribution of phases in heterogeneous microstructure has a large effect on the final mechanical properties of the investigated materials. Microstructure of the system is described by means of small angle neutron scattering (SANS). SANS provides a unique possibility of non-destructive characterization of secondary particles and all material's heterogeneity.

K e y w o r d s: molybdenum disilicide, small angle neutron scattering (SANS), microstructure parameters

1. Introduction

Molybdenum disilicide is an excellent matrix material for application as high temperature structural component, mainly because of its high melting point of 2030 ℃ and excellent oxidation resistance [1]. Mechanical properties of $MoSi_2$ could be improved by the addition of ceramics strengthening, for example: SiC and Si_3N_4 particles, nano SiC particles. They are thermodynamically compatible with $MoSi_2$, have high elastic moduli and they are available as particles, fibres, or whiskers [2, 3]. Composite materials can be considered as multiphase systems consisting of matrix with particles dispersed within its bulk. Size, morphology, volume fraction and spatial distribution of secondary phases affect final properties of dispersion-strengthened materials.

The conventional methods do not allow obtaining global microstructure parameters, such as volume fraction of particles, their distribution in volume unit, morphology and size distribution throughout the bulk of the investigated material. Theoretical knowledge supported by a number of studies suggests that the phase distribution in a heterogeneous microstructure greatly influences the final mechanical properties of the material [4]. The intention, however, is not only to describe the microstructure but also to interpret it in relation to the material properties. Depending on precision of such interpretation, it would be possible to choose and/or to determine the chemical composition and fabrication procedure of materials with required properties.

Small angle neutron scattering (SANS) method is well known to be suitable for such microstructure characterization. In contrast to direct imaging techniques like SEM, neutron waves scattered from material represent its microstructure as Fourier image of the material heterogeneities. As a result, scattering from large-scale features like pores or particles of secondary phase in composite ceramics give rise to scattering into very small angles related to the scattering vector magnitude, Q, and wavelength, λ, as $Q = 4\pi\theta/\lambda$, where 2θ is the full scattering angle. For the comprehensive review of the SANS theory, see [5, 6] and references therein. Application of SANS in materials research is often restricted due to problems with multiple scattering and high resolution required, both arising from typically broad size range of heterogeneities reaching 1 μm or more, as is the case of ceramics composites. In this paper, we show that the high resolution SANS

*Corresponding author: tel.: +421 55 7922411; fax: +421 55 7922408; e-mail address: bballokova@imr.saske.sk

technique using double-crystal diffractometer arrangement [7] can be used instead of the more common collimator system to overcome this problem. We have applied this technique to characterize microstructure of several $MoSi_2$ based materials of technological interest.

2. Experimental materials and methods

2.1. Materials

The materials studied in the present work were prepared by powder metallurgy technique of controlled reaction sintering in argon atmosphere.

The starting material was prepared in the Fraunhofer Institut für Fertigungstechnik und Angewandte Materialforschung in Dresden, Germany, according to the patent [8, 9]. The procedure is based on high energy milling (HEM) of coarse grained (grain size between 100 and 500 μm) Mo and Si powders of high purity. After milling for several hours in argon atmosphere in the planetary mill "Pulverisette 5" (made by Fritsch, Germany), highly dispersed powder mixtures were obtained. During preparation of the composites ceramic dispersoid particles (SiC, Si_3N_4) were being added into the matrix in various volume fractions. Finally, the milled mixtures were compacted by pressing to high density (over 95 % of the theoretical density) and subsequently subjected to pressureless reaction sintering. The sintering was carried out in vacuum at 1500 ℃.

$MoSi_2$ based materials were supplied in the form of disks with diameter of 50 mm and thickness of 5 mm. The disks were cut to obtain the bending bars with dimensions of $3 \times 4 \times 42\,\mathrm{mm}^3$.

2.2. SANS experiment

The SANS measurements were carried out at the double-crystal diffractometer DN-2 at Nuclear Physics Institute Řež [7] using the mean neutron wavelength $\lambda = 0.21$ nm. This type of instrument employs double diffraction of neutrons on elastically bent perfect Si crystals in non-dispersive arrangement in order to achieve high angular resolution even with a wide and divergent neutron beam. Consequently, the instrument is more efficient in high-resolution experiments than collimator facilities. Moreover, the high resolution is achieved with a relatively short neutron wavelength. This reduces problems connected with multiple scattering encountered when measuring thick samples containing large particles. The resolution and range of the scattering vector magnitude, Q, can be tuned by varying bending radii of the Si crystals, so that they match the expected size of measured inhomogeneities. In our case, measurements were carried out in three overlapping Q ranges spanning all together the interval 0.0011–0.1 nm^{-1} (see Fig. 1). This corresponded to approximately 10–1000 nm on the size scale. The measurements in the shortest Q range were measured twice for different sample thickness in order to evaluate the effect of multiple scattering.

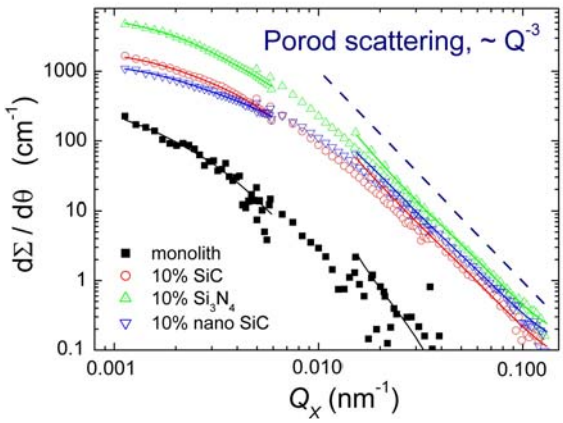

Fig. 1. Measured scattering curves (points) for selected materials are composed from three data sets at different Q-ranges for each material. The model scattering curves (lines) were obtained by fitting single set of model parameters simultaneously to all the three Q-ranges. The dashed Q^{-3} curve indicates the slope of Porod scattering for the used "infinite-slit" experimental arrangement.

2.3. Evaluation of experimental data

After a standard preliminary data reduction including background subtraction, corrections on absorption and calibration of intensity and angular scales, the resulting scattering curves were fitted to model parameters using the program SASProFit [10, 11]. The model used to describe the microstructure of our materials was composed of homogeneous spherical particles with the distribution of radii represented by a set of 10 cubic spline functions. Random spatial distribution of spheres was assumed so that inter-particle interference effects could be neglected. Such an assumption is justified for systems of non-interacting particles with low volume fractions. We also assume the validity of the first Born approximation, which implies the limit for the maximum radius of particles, $R_{\max} < 1/(2\Delta\rho\lambda)$, where $\Delta\rho$ is the scattering contrast defined as the difference between scattering length densities of the particles and matrix. Adequacy of these approximations in our case is discussed later. The model scattering function can be then expressed as [6]:

$$S(Q) = (\Delta\rho)^2\, t \int_{R_{\min}}^{R_{\max}} D(R)\, V(R)\, |F(RQ)|^2\, \mathrm{d}R, \quad (1)$$

where t is the sample thickness, $F(x)$ is the form-factor of a sphere,

$$F(x) = 3\frac{\sin(x) - x\cos(x)}{x^3}, \qquad (2)$$

$V(R)$ stands for the volume of a sphere with radius R and $D(R)$ is the distribution of sphere radii, R,

$$D(R) = R_{\max}^{-1} \sum_{i=1}^{n} p_i B_i \left(R/R_{\max}\right). \qquad (3)$$

$D(R)$ is normalized so that its integral equals to $\phi(1-\phi)$, where ϕ is the volume fraction of particles. $B_i(x)$ are cubic spline functions used to model size distribution on a fixed interval of particle radii $R_{\min} \ldots R_{\max}$. The p_i and $R_{\max}$ are free parameters to be determined by the least-square fitting.

Equation (1) describes theoretical differential cross-section for single scattering in pinhole geometry. In the case of double-crystal instruments, only the horizontal component of the scattering vector is resolved and the measured intensity is integrated along its vertical component. For isotropic materials as in our case, this integration does not bring about a principal loss of information provided that appropriate smearing procedure is applied to the model scattering function. Actual model scattering curve fitted to experimental data therefore included also smearing by the instrument resolution function, as well as corrections on multiple scattering and 3rd order harmonics wavelength $\lambda/3$, which contaminates neutron beam reflected from the Si 111 monochromator. Details of the whole data analysis procedure can be found in [11].

Given the assumed particle shape and $D(R)$ obtained by fitting the experimental data, we could evaluate various integral parameters characterizing the material microstructure, such as mean radius, volume fraction or specific surface of particles. Equation (1) implies that we need to know the scattering contrast $\Delta\rho$ of investigated particles in order to evaluate their volume fraction from scattering intensity. For this purpose, we have calculated scattering length densities using known mass densities of the phases present in the material and tabulated scattering lengths of constituent nuclei (see [12, 13]). These values are summarized in Table 1.

Table 1. Mass densities, d, scattering densities, ρ, and scattering contrasts, $(\Delta\rho)^2$, with respect to the $MoSi_2$ matrix for constituent phases

	d (g cm^{-3})	ρ (10^{10} cm^{-2})	$(\Delta\rho)^2$ (10^{20} cm^{-4})
$MoSi_2$	6.15	3.65	–
SiC	3.19	5.17	2.31
Si_3N_4	3.187	6.82	10.05
SiO_2	2.20	3.47	0.03
Voids	–	–	13.32

3. Results and discussion

The measured scattering curves and corresponding model curves for selected materials are shown in Fig. 1. The data measured at different Q regions on the same material obviously do not overlap due to instrumental effects. However, the model scattering curves include the instrumental effects as well and could therefore be fitted to the data in all the three Q-ranges simultaneously using the same set of model parameters. Measurements at different Q-ranges are thus consistent and provide information about sample microstructure within the wide range of particle radii of about 10 to 1000 nm. In all cases, the asymptotic Porod scattering at large Q is well defined. This permits to evaluate specific surface of phase boundaries independently of their shape. Note that the Porod scattering is proportional to Q^{-3} for the slit-smeared geometry of our experimental arrangement, as opposed to the Q^{-4} dependence commonly observed in the pinhole geometry.

Integral characteristics obtained from SANS data are summarized in Table 2. It has to be noted that the errors given in the table represent standard deviations resulting from fitting procedure and do not include systematic errors. The systematic errors can be caused by uncertainties in specific masses of the constituents or in sample thickness, by particle shapes other than the model (globular) one, by contamination of the neutron beam by neutrons of other wavelengths, etc. Measurements on standard samples (monodisperse polystyrene spheres) show that systematic errors in determination of absolute intensities and hence volume fractions and specific surfaces can reach about 10 %.

In order to assess the sensitivity of the obtained results to the shape of model particles, we have repeated the procedure using the model of elongated particles represented by ellipsoids with aspect ratio $c/a = 5$. As may be seen from Table 2, resulting volume fractions and specific surfaces were the same within experimental errors. This confirms that these integral parameters are suitable for characterization of polydisperse systems with variety of particle shapes like in our case. On the other hand, it also means that scattering data from such a system cannot provide unambiguous information about particle shape.

3.1. Volume fraction and specific surface

Comparison of nominal and measured volume frac-

Table 2. Volume fractions, ϕ, and mean specific surface, $\langle\sigma\rangle$, of secondary particles in the studied materials. The fractions of SiC and Si_3N_4 were evaluated after subtraction of scattering from the first (monolith) sample. The indicated errors are the standard deviations obtained from the fitting procedure. The "sph" and "ell" suffixes refer to the models of spheres and ellipsoids ($c/a = 5$), respectively

	ϕ_{sph} (%)	ϕ_{ell} (%)	$\langle\sigma\rangle_{sph}$ (μm^{-1})	$\langle\sigma\rangle_{ell}$ (μm^{-1})
$MoSi_2$ – voids	0.13 ± 0.03	0.17 ± 0.05	0.05 ± 0.02	0.05 ± 0.04
$MoSi_2$ – 5 % SiC	5.6 ± 0.3	5.5 ± 0.3	0.92 ± 0.1	0.95 ± 0.14
$MoSi_2$ – 10 % SiC	11.2 ± 0.4	11.1 ± 0.4	1.9 ± 0.2	2.1 ± 0.3
$MoSi_2$ – 15 % SiC	24.7 ± 0.6	25.0 ± 0.5	4.0 ± 0.2	4.6 ± 0.4
$MoSi_2$ – 10 % Si_3N_4	7.4 ± 0.2	7.4 ± 0.2	0.92 ± 0.05	1.02 ± 0.07
$MoSi_2$ – 10 % nano SiC	12.2 ± 0.3	12.2 ± 0.4	2.6 ± 0.2	3.0 ± 0.3
$MoSi_2$ – voids after creep, 800 °C, 100 MPa	0.11 ± 0.02	0.14 ± 0.03	0.05 ± 0.03	0.06 ± 0.04

tions of secondary phases shows systematic deviations. For the 5 % and 10 % SiC particles, the measured fractions are only slightly higher and can be at least partly explained by the above-mentioned systematic errors. However, the difference is much more significant for the 15 % SiC and Si_3N_4 particles. The specific surfaces are consistent with this observation, namely the surface for the 15 % SiC sample is more than twice larger than for 10 % SiC.

The excess volume fraction and specific surface in SiC composites can be due to other phases present in the material. Possible candidates are pores and glassy SiO_2 particles, which were identified in the monolith as well as in the composites by EDX. Although the observed volume of SiO_2 particles is rather high, they contribute very little to scattering intensity due to their very low scattering contrast with respect to the $MoSi_2$ matrix (see Table 1). On the other hand, scattering contrast of pores is two orders of magnitude stronger. Moreover, the pores are created near the phase boundaries. Their volume therefore increases with the volume of secondary particles and they also increase the effective size of the particles as seen by neutrons. This effect is probably responsible for systematically higher volume fractions resulting from SANS. Unfortunately, as long as the size of pores or other phases is roughly the same as that of the secondary particles, it is impossible to distinguish them on the scattering curves.

Both pores and SiO_2 particles are also present in the monolithic $MoSi_2$ with no secondary phase. Corresponding volume fraction 0.13 % in Table 2 has been evaluated under the assumption that scattering from this material is entirely due to the pores. Probably, this number also includes scattering from the glassy silica phase, which is clearly visible in higher volume on the micrographs (Fig. 2) but has much lower contrast for neutrons when compared to pores.

For illustration, we include a microstructure of $MoSi_2$ composite with 10 % of nano SiC as the secondary phase, Fig. 2a. The secondary phase in the mater-

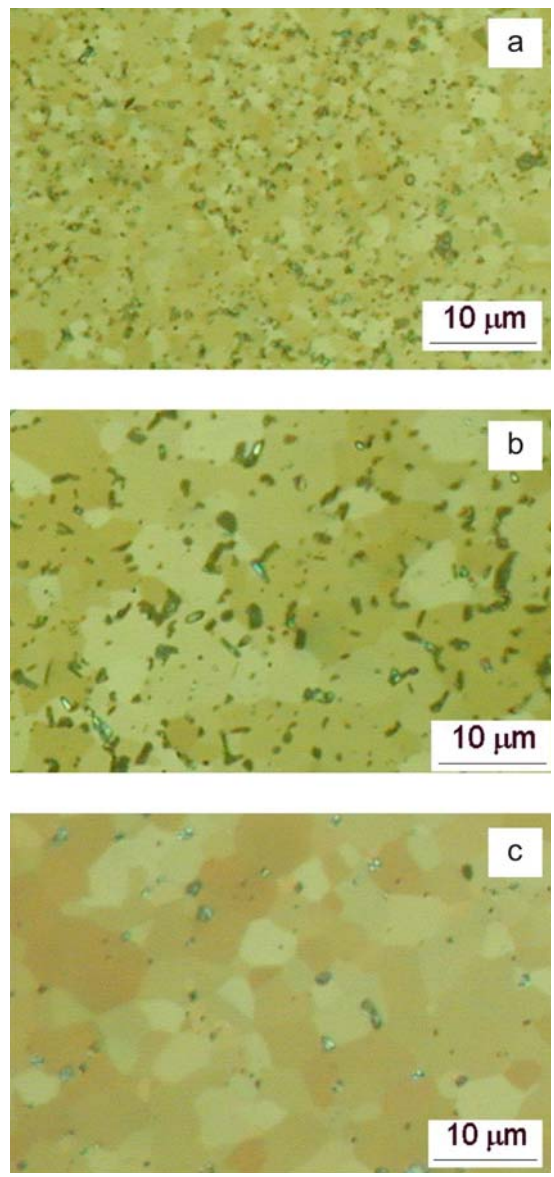

Fig. 2. Microstructure of investigation materials, optical microscope, polarized light: a) $MoSi_2$ + 10 % nano SiC, b) $MoSi_2$ + 10 % Si_3N_4, c) $MoSi_2$.

ial with 10 % Si_3N_4 tended to form particle clusters (see Fig. 2b). In such a case, the model of randomly distributed non-interacting particles is no longer valid. As a result of inter-particle correlations, the scattering intensity becomes usually lower in the small-Q region, which leads to the underestimation of particle size and volume fraction. This explains that only in this material the particle volume fraction is lower than nominal, namely 7.4 %.

In monolithic $MoSi_2$ with no secondary phase, the fraction of 0.13 % represents the content of pores and glassy silica phase (Fig. 2c). To illustrate the point better, the monolithic $MoSi_2$ after creep testing at temperature of 800 ℃ and load of 100 MPa was analysed, too. No significant changes in volume fraction of pores and amorphous phase were found after creep, the value was 0.11 %.

3.2. Size distribution of secondary phase particles

As opposed to volume fractions and specific surfaces, the size distribution evaluated from SANS data naturally depends on the choice of model particles. Ideally, their shape should match as close as possible the shape of real particles found in the material. This is obviously not possible in polydisperse systems with wide variety of particle shapes. In such a case, the model particles represent merely an effective scale with which the size of particles is measured. Then the size distribution $D(R)$ has to be interpreted as a distribution of spheres (or any other model shape), which gives rise to the same scattering as the real system. Consequently, the profile of $D(R)$ would depend on the choice of model particle shape. Nevertheless, such an artificially defined quantity is often sufficient and adequate as microstructure characteristics, when studying changes of material microstructure as a function of parameters of preparation and post-preparation treatment, which is often the task in materials research. By definition, the $D(R)$ distribution describes *partial volume fractions* rather than *number of particles*, as is usual in SEM. Since the scattering cross-section of a particle is proportional to R^4, SANS is considerably more sensitive to large particles (or particle clusters), which means that the distribution with respect to volume represents better the reality reflected by neutron scattering.

The distributions of sphere radii, $D(R)$, obtained from our SANS measurements are shown in Fig. 3.

In all the composite materials, the radii of the secondary phase particles ranged from 20 nm up to 1000 nm. As expected, the distribution of nano SiC particles (see Fig. 2a) shows significantly lower fraction of large particles compared to other materials. The curve for the material with 10 % Si_3N_4 broadened towards large radii, which is consistent with the microscopic observations of particle clusters. All other curves have maxima around 100 nm. Referring to the previous discussion, it should be pointed out that the extent of $D(R)$ to small radii does not necessarily mean the presence of such small isolated particles, but can be caused by irregular shape of phase boundaries with higher specific surface than spheres of the same size and volume.

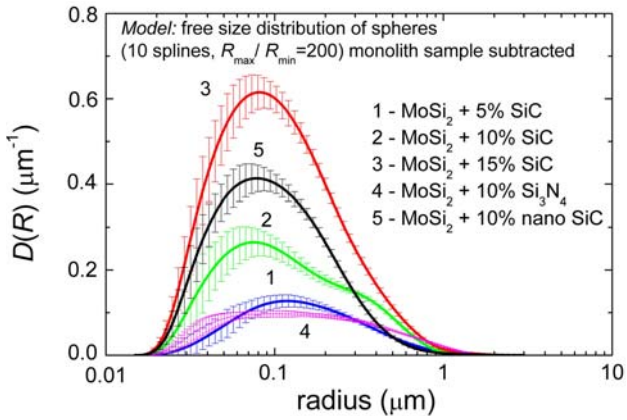

Fig. 3. Size distributions of secondary phase particles.

As seen from both the micrographs (Fig. 2) and size distributions (Fig. 3), the condition for validity of the first Born approximation, $R_{max} < 1/(2\Delta\rho\lambda)$, is obviously satisfied in our experiment. For example, R_{max} should be less than about 7.5 μm for the Si_3N_4 particles and $\lambda = 0.21$ nm. However, it would not be the case if measurement is carried out on a collimator SANS facility, where high resolution regime with $Q_{min} \sim 10^{-3}$ nm^{-1} would require the use of cold neutrons with much longer wavelength.

4. Conclusions

From the results of microstructure evaluation of monolithic $MoSi_2$ and $MoSi_2$ based composites by SANS, following conclusions can be drawn:

1. High resolution SANS is a suitable method for quantitative study of large scale (10 nm – 1 μm) microstructure of ceramics composites. However, it has to be combined with imaging methods and phase analysis in order to interpret the scattering data unambiguously. The added value of SANS is then non-destructive determination of statistically relevant micro-structural characteristics, which represent macroscopic volume of bulk material. These characteristics can be thus directly related to other physical properties of the material and/or the parameters of preparation and post-preparation processes.

2. Volume fraction and specific surface of secondary phase particles determined from SANS data were

found to be practically independent of the choice of model particle shape.

3. Glassy silica particles observed in microscopic images in significant volume fractions have nearly no effect on neutron scattering due to their very low scattering contrasts in the $MoSi_2$ matrix. However, they might be partly responsible for weak scattering from the monolithic materials. The low contrast is advantageous for evaluation of measurements on composite $MoSi_2$, because contribution from silica particles can be neglected and only the two other phases (secondary phase particles and pores) have to be considered in data analysis.

4. The measured data do not allow distinguishing multiple phases in the studied materials, although pores have been observed by imaging methods in addition to the secondary phase. Residual porosity contributes at least partly to the scattering from monolithic materials. By neglecting possible contribution of the SiO_2 particles, we could evaluate the upper limit for the volume fraction of the residual porosity to 0.1 vol.%.

5. Volume fractions of secondary phase in composite materials determined by SANS are close to the nominal ones, although they are systematically higher for the SiC composites. Scattering by pores is a plausible explanation of this deviation. On the contrary, the volume was lower than nominal for the Si_3N_4 phase, which is known to form large aggregates. The model of non-interacting spherical particles is then inadequate and leads to apparently larger particle radii and lower volume fractions. This is in agreement with the observed size distribution.

Acknowledgements

This research project has been supported by the European Commission under the 7th Framework Programme through the 'Research Infrastructures' action of the 'Capacities' Programme, Contract No: CP-CSA_INFRA-2008-1.1.1 Number 226507-NMI3 and project VEGA No. 2/0105/08. Support from the Czech Ministry of Education (No. MSM2672244501) and Czech Academy of Sciences (No. AVOZ104805505) is also appreciated.

References

[1] PETROVIC, J. J.—HONNELL, R. E.—MITCHELL, T. E.: Ceram. Eng. Sci. Proc., *12*, 1991, p. 1633.
[2] GAC, F. D.—PETROVIC, J. J.: J. Am. Ceram. Soc., *68*, 1985, p. 200.
[3] SHAW, L.—ABBASCHIAN, R.: J. Am. Ceram. Soc., *78*, 1995, p. 3129.
[4] KOHUTEK, I.—BESTERCI, M.—KULU, P.: Acta Metal. Slovaca, *4*, 1998, p. 123.
[5] KOSTORZ, G.: In: Neutron Scattering (Treatise on Materials Science and Technology). Ed.: Kostorz, G. New York, Academic Press 1979, p. 227.
[6] FEIGIN, L. A.—SVERGUN, G. I.: Structure Analysis by Small-Angle X-ray and Neutron Scattering. Ed.: Taylor, G. W. New York, Plenum Press 1987.
[7] STRUNZ, P.—ŠAROUN, J.—MIKULA, P.—LUKÁŠ, P.—EICHHORN, F.: J. Appl. Cryst., *30*, 1997, p. 844.
[8] SCHOLL, R.—BÖHM, A.—KIEBACK, B.: Material Science and Engineering, *A261*, 1999, p. 204.
[9] SCHOLL, R.—KIEBACK, B.: Patent DE 44 18 598 A1
[10] http://neutron.ujf.cas.cz/SAS
[11] ŠAROUN, J.: J. Appl. Cryst., *33*, 2000, p. 824.
[12] SEARS, V. F.: Neutron News, *3*, 1992, p. 26.
[13] http://www.ncnr.nist.gov/resources/sldcalc.html